

Revisiting maximum bow force with precise empirical data

Robert Mores

University of Applied sciences Hamburg, 22081 Hamburg, E-Mail: robert.mores@haw-hamburg.de

The maximum bow force defines the transitional point between Helmholtz regimes and bifurcation regimes. Schelleng (1971), Askenfelt (1989), Schumacher (1993) and Schoonderwaldt et al. (2008) formulated—in different ways—how the maximum bow force relates to bow velocity, relative bow-bridge distance, string impedance and friction coefficients. Related measurements at the respective regime transitions cover a diverse scenario of bowing machines and stringed instruments. So far, the empirical data does not clearly support either of the theories in a general way. A low-friction bowing pendulum has been constructed to allow precise measurement of relevant bowing parameters. Two cellos are measured across all strings for three different bow-bridge distances. The empirical data proves that none of the previous theories holds but a combination of two of them. The result is confirmed by supplementary measurement of the friction coefficients, while in the earlier publications these have only been estimated.

I. INTRODUCTION

The maximum bow force at which Helmholtz motion can be sustained has been investigated several times. Schelleng (1971) suggested

$$F_{\max} = \frac{Z \cdot v_B}{(\mu_S - \mu_D) \cdot \beta} \quad (1)$$

where Z is the characteristic translational impedance of the string, v_B is the bow velocity, μ_S and μ_D are the static and the dynamic friction coefficients, and β is the fractional bowing position with respect to the bridge. He considered μ_D to be velocity dependent but treated the friction difference $\mu_S - \mu_D$ as a constant.

Later, Askenfelt (1989) introduced an additional factor of two¹

$$F_{\max} = \frac{2 \cdot Z \cdot v_B}{(\mu_S - \mu_D) \cdot \beta} \quad (2)$$

where the friction difference (μ_S and μ_D) is treated as a constant as well. In a much later publication together with Schoonderwaldt and Guettler (2008) he used the asymptotic μ'_D instead of μ_D . μ'_D stands for the μ at a relative slip velocity $z = v_B / \beta \rightarrow \infty$.

$$F_{\max} = \frac{2 \cdot Z \cdot (v_B + \beta \cdot z_0)}{(\mu_S - \mu'_D) \cdot \beta} \quad (3)$$

where z_0 is introduced as a necessary minimum velocity offset for z .

¹ Schuhmacher later references to a footnote in Schelleng's publication saying that a factor of two would make sense.

Chronologically between these two publications, Schuhmacher (1994) used a velocity-dependent function to weight the friction difference.

$$F_{\max} = \frac{2 \cdot Z \cdot |v_B|}{(\mu_S - \mu'_D) \cdot (1 - f(v_S)) \cdot \beta} \quad (4)$$

where v_S is the slip velocity, $v_S = v_B \cdot (1 - 1/\beta)$, and the weighting function $f(v)$ is unknown.

Taking a closer look at these definitions, some of the authors refined their model by including the rotational (or torsional) admittance of the strings. Schelleng and Schuhmacher both used the factor $(1 - \zeta)^{-1}$ to describe the lowering of resistive force, with ζ being the relation of translational to rotational impedance, $\zeta = Z/Z_r$. While Schumacher used this extra term for data fitting, Schelleng did not. Schoonderwaldt also used this correction term for data fitting. So Z in Eqs. (1) through (4) optionally reads $Z/(1 - \zeta)$ instead of Z . Optionally because none of the authors claimed the relevance of torsion in such a confident way that they would have introduced the term in the formula in the first place.

While Schelleng did not provide empirical data to confirm Eq. (1), Askenfelt used a setup for in-situ measurements for bow force F_B , v_B and β . Based on measurements on a steel pin he assumed the friction difference to be constant in the range of $\mu_S - \mu_D = 0.2 \dots 0.3$. Using this assumption, the values for F_{\max} as predicted by Eq. (2) were 1.5 to 2 times higher than the measured values, for low and high bow velocities, respectively (Askenfelt, Fig. 4e). The measured values are not only well outside the predicted range but they are also uncertain in terms of bow velocity (the total span implies a factor of 1.5 to 2). Askenfelt did not consider rotational admittance. In order to proof Eq. (3), Schoonderwaldt et al. used Cronhjort's converted daisy wheel printer (1992). The measured bow force limits confirm the velocity term in Eq. (3) and the results are in agreement with Schuhmacher's findings. The introduction of the velocity term results in a convincing modelling improvement when comparing the limits derived from Eq. (2) against those derived from Eq. (3) in the Schelleng diagram across eleven different β and four different bow velocities. From these measurements on a violin steel D string mounted on a monochord they derived the estimate for $\mu_S - \mu_D = 0.38$ to 0.6 at $v_B = 5$ to 20 cm/s, using Eq. (2), and $\mu_S - \mu_D = 0.51$ to 0.67 at $v_B = 5$ to 20 cm/s, using Eq. (3). Measurements on friction coefficients are not reported. However, the estimates for $\mu_S - \mu_D$ now vary widely and will not become clearer when consulting other researchers. Reports on just the static friction vary widely, e.g. from Saunders' $\mu_S = 0.2$ (1937) to Lazarus' astonishing $\mu_S = 1.4$ (1972).

Schuhmacher did the most careful work to respect the rotational component as he disassembled strings to determine the inertia density and subsequently the rotational admittance, but the finding do not support his model, since no measurements of the necessary friction coefficients are reported. Finally, there are three uncertainties with the existing models: the factor 2 in the nominator, the velocity term, and the rotational admittance.

II. METHOD

This research seeks to affirm existing models and to resolve the uncertainties by precise measurements. The proposed precision pendulum allows to measure bow force, bow velocity and bow-bridge distance, but also the tractive force that is necessary to move the bow and to overcome friction. Tractive force and bow force are measured in a strictly orthogonal arrangement so that friction coefficients can be derived, both static, μ_S , and velocity- dependent, μ_D . Regressions are used for the inductive step towards existing models and the related fit factors are used to derive suggestions.

III. INSTRUMENTATION

A. Pendulum

This empirical study employs a bowing pendulum which allows strictly straight bowing movements for real bows and string instruments of any size. Instead of a motor the system uses gravity to create a constant force for bow traction. The moving mass at which the bow is mounted emulates the musician's arm, while a damping unit emulates the mechanical impedance of the musician's arm. The mechanical impedance of the driving force and the impedance of the stick-slip process are in equilibrium at a bow velocity determined by the stick-slip process itself. Other researchers used a motor to drive the bow and the bow velocity was usually predetermined and selectively fixed. The friction of the system is very low (<0.5 N) and can be measured and taken into account during instrumentation. In the mechanically strictly orthogonal arrangement of bow force and tractive force, these two parameters can be measured independently from each other and independent from stroke direction and bow velocity. The total maximum errors for worst case instrumentation conditions across the entire range is indicated in Table I and confirmed against physical reference. In terms of dynamic response, the 90% rise-time is less than 10 ms for all parameters and data are arranged in tuples of 12.5 ms. The pendulum's construction principle, employed hardware, and operational ratings are reported (Mores, 2015).

Table I. Maximum error ratings of the bowing pendulum instrumentation.

Physical property		Maximum error
s_B in cm	bow position	± 0.18 cm
v_B in cm/s	bow velocity	± 0.025 cm/s
F_t in N	tractive force	± 0.15 N ± 1 %
F_B in N	bow force	± 0.11 N

B. Typical raw data

The four open strings (quality range from medium to high) on two celli (student level and soloist level) were measured at $\beta = 1/8, 1/16, \text{ and } 1/32$ and at bow velocities in the range from 0.3 cm/s to 10 cm/s. With the tractive force being fixed and the bow force ramping within a narrow range the adaptive driving will reveal the likeliness of the stick-slip process to reside either regime, Helmholtz motion or bifurcation. This can be observed in the populations of bow force F_B versus velocity v_B , see Fig. 1.

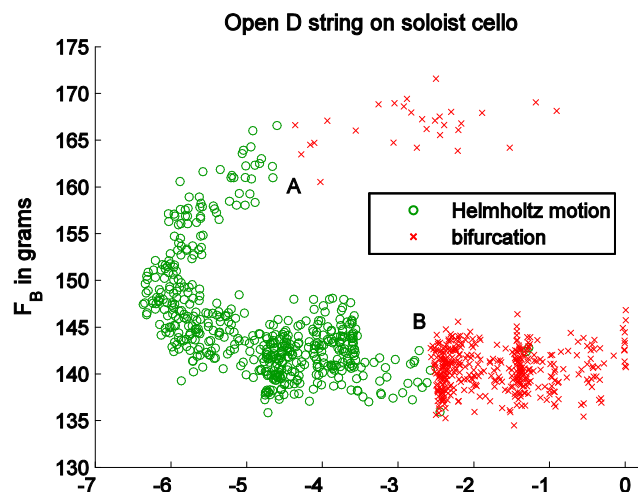


FIG. 1. Raw data examples of bow force versus bow velocity. Each entry represents 12.5 ms of bowing. Gaps are not only observable between regimes, but also within regimes, Helmholtz motion and bifurcation.

The populations of these two regimes are well separable. In many cases, the classes can be automatically separated by Support Vector Machines (SVM) with three support vectors, region A in Fig. 1, and usually less than some 20 support vectors, region B. Interestingly, gaps also appear within regimes, both Helmholtz motion and bifurcation. Such step-wise bow velocity increments or decrements are defined by the stick-slip interaction, since the potential tractive force is defined by constant gravity and adaptive impedance while the bow force is gradually ramped up or down.

IV. RESULTS

A. Maximum bow force and friction

Examples of extracted thresholds across different β are given in Fig. 2. As expected by all of the mentioned equations, v_B and β are both major predictors for the maximum bow force.

Fig. 3 presents the extracted maximum bow forces for both celli normalized to $\beta = 0.1$ and $Z = 1$ kg/s. The figure represents measured data and related linear regressions. It also shows the trend lines suggested by the existing models. Clearly, among the existing definitions Schelleng's approach is the one that comes closest to the linear regression of this empirical data set, see the trend line denoted with Eq. (1) in Fig. 3. The factor 2 given in Eqs. (2) through (4) cannot be confirmed by our data set, see results plotted for Eqs. (2) and (4). The trend line for Eq. (4) uses the measured dynamic friction μ_D to represent the velocity term proposed by Schuhmacher.

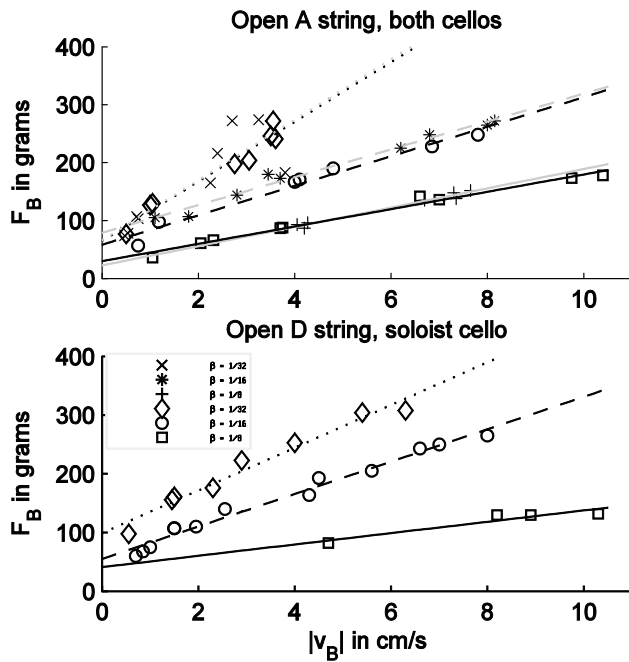


FIG. 2. Measured maximum bow force for three different relative bridge distances and related linear regressions. Top: measurements on the open A strings for a soloist cello (\square , \diamond , \circ) with regressions (black) and for a student cello (\times , $*$, $+$) with regressions (grey), strings have similar translational impedance (<3% difference). Bottom: measurement results for the soloist cello.

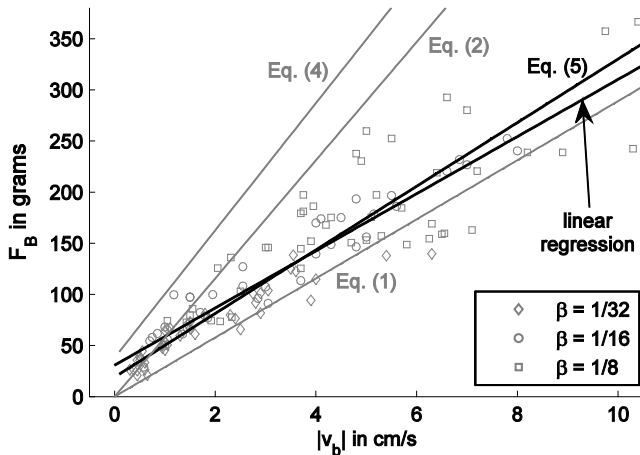


FIG. 3. Measured maximum bow force for three different relative bridge distances and related linear regressions normalized to $\beta = 0.1$ and $Z = 1$ kg/s for the soloist cello. Trend lines denoted with Eqs. (1), (2) and (4) represent existing models, trend line denoted with Eq. (5) represents the model proposed here.

The introduction of the velocity dependent dynamic friction μ_D is a reasonable option to consider for modelling. The dynamic friction was measured on the same instrumentation setup. The string was dampened to avoid Helmholtz motion, while the resulting sound was noise alone without any perceivable pitch. Bow force and relative bridge distance were varied across the same range as for the extraction of maximum bow force. See Fig. 4 for results. The static friction was also measured at 30 instances of stick to slip transitions in a single shot operational mode (pitch below 2 Hz), $\mu_S = 0.6426 \pm 0.0015$. Static friction was not taken into

account for the hyperbolic regression of μ_D to avoid biased wrong assumptions. As a result, μ_S is in good agreement with the derived μ_D at the slip velocity $v_S = 0$. The asymptotic $\mu'_D = 0.346$ results from numeric optimization, $R^2 = 0.88$. Finally, dynamic friction is described by $\mu_D = \mu'_D + 1/(0.512 \cdot v_S + 3.063)$.

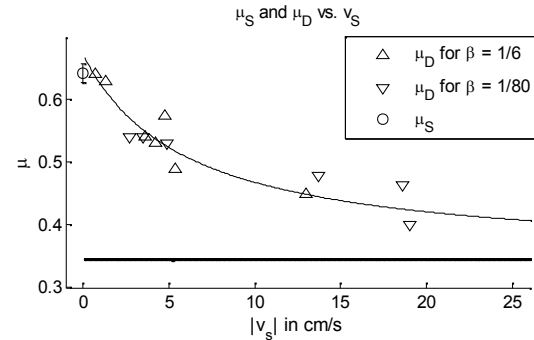


FIG. 4. Static friction coefficient $\mu_S = 0.6426$ (\circ) with standard deviation ($N = 30$), velocity-dependent dynamic friction coefficient μ_D (∇ , Δ) with hyperbolic regression ($R^2 = 0.88$), and asymptotic dynamic friction coefficient μ'_D , line at 0.346.

As a suggestion, the velocity dependent dynamic friction is combined with Schelleng's initial approach,

$$F_{\max} = \frac{Z \cdot |v_B|}{(\mu_S - \mu'_D) \cdot (1 - f(v_S)) \cdot \beta} \quad (5)$$

For the trend line in Fig. 3 the term $(\mu_S - \mu_D)$ is used instead of the term $(\mu_S - \mu'_D) \cdot (1 - f(v_S))$ because of the existing empirical data for μ_D . The equivalence $v_S = v_B \cdot (1 - 1/\beta)$ facilitates indexing the relevant μ_D . This is necessary here, because the slip velocity v_S under Helmholtz regimes cannot directly be measured with the given instrumentation setup whereas v_B can be measured.

B. Results from regression

Table II summarizes the results. R^2 for the linear regression is above 0.84 for both instruments. For comparison, Eqs. (1) through (4) are used as a reference for calculating residuals. The resulting R^2 for each case indicates how well or how poor existing models fit the data. While R^2 is well above 0.5 for Eq. (1), it is well below zero for both, Eqs. (2) and (4). These predictions are clearly out of range. R^2 for Eq. (5) is very close to R^2 obtained by linear regression.

Table II. Fit results for maximum bow force, without rotational admittance for the existing models.

	R^2 for data versus Eq. (1)	R^2 for data versus Eq. (5)	R^2 1 st order regression	R^2 2 nd order regression
Cello	0.699	0.832	0.843	0.847
Soloist	0.605	0.821	0.857	0.863

By visual inspection of Fig. 3, Eq. (5) even agrees better with the data than the linear prediction for low bow velocity. One could argue for a second order fit. However, there is not much to gain with a second order fit, see Table II (second order fit is not shown in Fig. 3). The spread in the data

caused by the regime transition hysteresis is still the main reason for a missing perfect fit. Any future modelling approach might start with a clearer definition of regime transitions before striving for precision.

One can argue that including the rotational admittance component facilitates a better fit. Using Schelleng's quoted $1/\zeta = 2.5$ (cello A string) to $1/\zeta = 3.0$ (cello C string), the resulting R^2 for the existing models do not really convince. $1/\zeta = 2.75$ is used for results in Table III.

Table III. Fit results for maximum bow force, with rotational admittance for the existing models.

Cello	R^2 for data versus Eq. (1)	R^2 for data versus Eq. (2)	R^2 for data versus Eq. (4)
Soloist	0.249	0.557	< 0
Student	0.095	0.662	0.252

To conclude, when screening the existing models, both in their plain version but also when extended by rotational admittance, only two of them roughly determine maximum bow force, i.e. Schelleng's plain model without the velocity term and without rotational admittance ($R^2 = 0.699$) and Askenfelt's plain model without velocity term but with rotational admittance ($R^2 = 0.662$). However, remember that Askenfelt did not propose to use rotational admittance.

On the other hand, extending Schelleng's plain model by the velocity term, as proposed by Schuhmacher, yields the best fit ($R^2 = 0.832$). Empirical data is mutually confirmed along this model since both have been measured, the parameters at regime transitions and the friction coefficients. After all, it seems valuable to revisit the proposed models with the given empirical data.

Another observation is that the assumption of a necessary z_0 in Eq. (3) is not supported by the data. The data clearly approaches $F_B = 0$ at $v_B = 0$. So one could argue that Eq. (5) introduced here should represent this. However, it might well be that the assumption of a hyperbolic progression of μ_D is wrong, see the junction between μ_S and μ_D and the progression at low bow velocity in Fig. 4. So an improved modelling might begin with adequately modelling μ_D .

V. DISCUSSION

The existing models for maximum bow force look similar at first sight, but imply a range of options, especially the option of using a velocity term in combination with the given friction, and the option of regarding rotational admittance. The empirical data here suggests to use the velocity term in Schelleng's model. However, this can only be a rough approach to what is actually happening at the contact point, because the slip velocity is not constant.

The empirical data however suggests not to consider rotational admittance. Using the term $(1 - \zeta)^{-1}$ with $\zeta = Z/Z_r$, as suggested by Schelleng, and used by Schuhmacher and Schoonderwaldt, implies that the lowering of the translational impedance is static. However, the frequencies differ for the two types of vibration, translational and rotational.

VI. SUMMARY

A bowing pendulum facilitates precise parameter extraction from bowing. Existing theories for the maximum bow force are revisited and the early theory of Schelleng comes closest to empirical data, especially when combined with a velocity term for the dynamic friction. The results are trustworthy because the friction coefficients are likewise determined by instrumentation whereas earlier publications based on rough assumptions.

REFERENCES

- Askenfelt, A. (1989). "Measurement of the bowing parameters in violin playing. II: bow-bridge distance, dynamic range, and the limits of bow force," *J. Acoust. Soc. Am.* **86**, 503–516.
- Cronhjort, A. (1992). "A computer-controlled bowing machine (MUMS)," *Quarterly Progress and Status Report of the KTH Stockholm (STL-QPSR)* **33**, 61–66.
- Lazarus, H. (1972). "Die Behandlung der selbsterregten Kippschwingungen der gestrichenen Saite mit Hilfe der endlichen Laplacetransformation," Ph.D. thesis, Technical University Berlin, cited in L. Cremer (1971), "Die Geige aus Sicht des Physikers," *Nachr. Akad. Wis. Göttingen II Math Physik, Kl 12*, 223–259, reprinted in *Benchmark Papers in Acoustics*, Vol. 5, edited by C. M. Hutchins, Wiley-Halsted, New York, 1975.
- Mores, R. (2015). "Precise cello bowing pendulum," in *Proceedings of the Third Vienna Talk on Music Acoustics*, 106 ff.
- Saunders, F. A. (1937). "The mechanical actions of violins," *J. Acoust. Soc. Am.* **9**, 81–98.
- Schelleng, J. (1971). "The bowed string and the player," *J. Acoust. Soc. Am.* **53**, 26–41.
- Schoonderwaldt, E., Guettler, K., and Askenfelt, A. (2008). "An empirical investigation of bow-force limits in the Schelleng diagram," *Acta Acustica united with Acustica* **94**, 604–622.
- Schuhmacher, R. (1994). "Measurements of some parameters of bowing," *J. Acoust. Soc. Am.* **96**, 1985–1998.
- Woodhouse, J., Schumacher, R. T., and Garoff, S. (2000). "Reconstruction of bowing point friction in a bowed string," *J. Acoust. Soc. Am.* **108**, 357–368.